

Review- Sensorless Techniques for Stabilization Control of Induction Motor Drives

Suha Sabah Shyaa

Technical College of Al-Mussiab, Al Furat Al-Awsat technical university, kufa, Iraq.

E-mail: suha.odah@atu.edu.iq

Received: 22 November 2023; Revised: 22 December 2023; Accepted: 23 June 2024

Abstract

The challenges inherent in achieving stability and efficient stabilization in an induction motor (IM) drive lacking sensors are significantly more pronounced than those encountered in a drive that incorporates sensors. This article comprehensively examines frequently recommended flux & speed estimators, like reduced-order and full-order state observers. Their sensitivity to parameter variations and their static and dynamic characteristics are the focal points of the evaluation. Instability is most severe at low speeds, rendering a resistance of the stator the most critical parameter. The current investigation explores a range of approaches to alleviate the impacts of this specific parameter.

Keywords: Estimation, induction motor, observers, sensorless, stability.

1. Introduction

Induction motor (IM) sensorless drives do not have a speed sensor. Due to the absence of a flux sensor, the drive is sensorless on both counts. It is necessary to estimate both flux and speed for sensorless control. Nonlinear dynamics complicate the task of designing a control system for sensorless operation. Low-speed performance is challenging. Some steps need to be taken in order to create a system that is both stable and functional. This paper reviews sensorless IM drive stabilization techniques and outcomes. This stabilization creates a well-damped system to prevent small-signal oscillations or ringing. Avoiding large-signal instabilities—situations in which torque and speed have opposite signs—which are frequent in the regeneration region, is even more crucial. In both scenarios, the flux-design estimator is critical. The theories and techniques of several

systems and control fields, including nonlinear systems theory, adaptive control, and parameter estimation, serve as a foundation for sensorless control.

The most important is the latter. If sufficiently designed, a wide variety of estimators can be used successfully. Analysis is necessary for success, and linearization is a helpful tool. This paper is divided into two sections for the remainder of it. Section II enhances the instructional value by initiating the conversation with the principles of flux estimation and vector control. During this procedure, the stability characteristics of both archetypal flux estimators—the voltage and current models are observed. These estimators are extensions to full- and reduced-order state observers. Speed estimation is added to the flux estimators. There is a discussion of the connections between various estimator types. Both analytical and preventative methods for the phenomenon are presented. Generally speaking, these techniques work with various kinds of estimators. There is a discussion of several techniques to lessen stator-resistance sensitivity. A few conclusions and recommendations for more study are included in Section III.

2. SENSORLESS VECTOR CONTROL FUNDAMENTAL

A. Induction Machine (IM) architecture

The equivalent circuit of the space-vector inverse model-T is demonstrated in Figure 1. The stator flux is used in the model [1] represented as $\psi_S^s = \psi_R^s + L_\sigma i_S^s$, where the symbol ψ_S^s represents stator flux space vector, ψ_R^s is rotor flux space vector, L_σ is leakage inductance and i_S^s is stator current space vector. As a complex state variable, the stator current is an alternative. The model allows for the same conclusions to be reached but at the cost of a marginally more complex theory, which is why we chose it. Nevertheless, saturation is extremely easy to simulate with the model[2] [3].

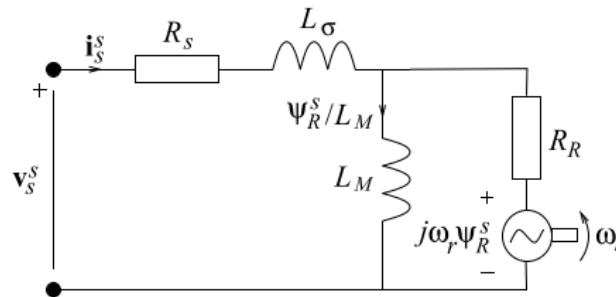


Figure 1. Inverse-T model of the IM equivalent circuit [2].

The T model is not recommended since it is overparameterized and contains both a stator and a rotor leakage inductance. The stator terminal quantities do not allow the unique identification of the two leakage inductances. An electrical dynamics of the IM in stator ($\alpha\beta$) coordinates are given by[4]:

$$\begin{aligned} L_\sigma \frac{di_S^s}{dt} &= v_s^s - (R_s + R_r)i_S^s + (a - j\omega_r)\psi_R^s \\ &= v_s^s - R_s i_S^s + E^s \end{aligned} \quad (1)$$

$$\frac{d\psi_R^s}{dt} = R_R i_s^s - (a - j\omega_r)\psi_R^s = E^s \quad (2)$$

The symbol v_s^s is stator voltage space vector, R_s & R_R are stator and rotor resistances, a is inverse rotor time constant and ω_r is electrical rotor speed. E^s represents the electromotive force of flux (EMF). A complex state variable's 2nd-order state-space system, i_s^s & ψ_R^s . In terms of real state variables, an electrical induction machine (IM) model is a 4th-order system. In addition, it is important to note that the speed ω_r is not only influenced by the electrical dynamics but is also regulated by the mechanical dynamics, which are of order one or higher. These mechanical dynamics interact with the electrical dynamics in a nonlinear manner through the process of multiplication by ω_r in equations (1) and (2). Furthermore, the electrical torque is also influenced by this relationship between the mechanical and electrical dynamics.

$$\tau_e = \frac{3n_p}{2K^2} I_m[(\psi_R^s)^* i_s^s] \quad (3)$$

Where τ_e is electrical torque

In this context, the symbol " n_p " represents the total number of pole pairs, whereas the symbol " K " specifies the constant associated with space-vector scaling & complex conjugate. Hence, it can be observed that the dynamics of the entire IM exhibit nonlinearity and at least order five. However, due to the slower nature of mechanical dynamics compared to electrical dynamics, ω_r is primarily acknowledged as a parameter. Consequently, equations (1) and (2) governing the electrical dynamics have linearity characteristics.

B. Fundamentals of Vector Control

An exponential decay rate of i_s^s in eq. (1) is $(R_s + R_R)/L\sigma$, while a rate of exponential decay ψ_R^s in eq. (2) is $a = R_R/L_M$. The rotor time constant and transient time constant are the terms used to refer to the inverses. These are usually measured in tens of milliseconds and hundreds of milliseconds. As a result, the rotor flux and stator current fluctuate on various time scales.

Consequently, there are differences in time scales between the rotor flux and stator current. A secret to getting a quick torque response is to control the current to maintain a constant flux while adjusting the torque (typically in a closed loop) [5][6]; this further reduces the effective transient time constant. This concept, field-oriented control, was created in the late 1960s [7][8]. The erstwhile term originates from aligning the dq frame, a synchronous coordinate system, with a space vector of flux. If a former is written in polar forms, such as

$\psi_R^s = \psi R e^{j\theta}$, then the dq transformation gives the dq-frame stator current

$$i_s = i_s^s e^{-j\theta} = i_{sd} + j i_{sq} \quad (4)$$

The substitution of equation (4) in equation (3) illustrates the direct relationship between torque and iq, where iq represents the current component responsible for generating torque in a direct current (DC) motor; precisely, it matches the armature current. Vector control enables the attainment of quick torque responses in DC motors, a feat that was previously deemed unachievable. The task of vector control would have been uncomplicated if the rotor flux had been simply measured. On the other hand, the measurement of flux is often not feasible, so a flux estimator, also known as an observer[9],[10] should generally be employed instead, with few exceptions yielding a flux estimate $\hat{\psi}_R^s = \hat{\psi} R e^{j\tilde{\theta}}$ ($\hat{\psi}_R^s$ is rotor flux estimate space vector). In equation (4), θ is then replaced by $\tilde{\theta}$, this

leads to the vector control system seen in Figure 2. The ability to estimate flux accurately, which will be further discussed in the following section, allows for minimal impact on drive performance. In contrast, inaccurate estimation of flow can lead to a decrease in performance and, in some cases, instability.

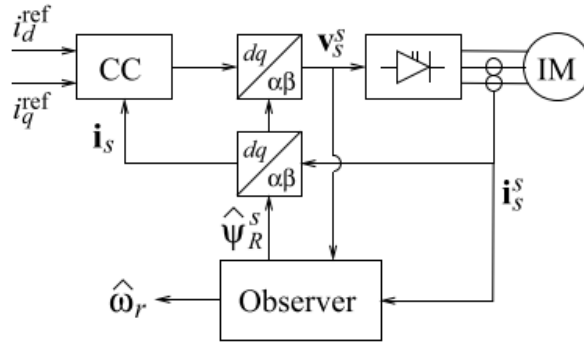


Figure 2. Synchronous-frame current controller (CC) and combined flux and speed observer (estimator) in an IM vector control system [11].

C. Sensorless Control Fundamentals

Sensorless control significantly increases the risk of poor performance and instability. The main challenge is estimating the flux without knowing the speed. In most sensorless schemes, voltage and current at the stator terminal are used to estimate flux and speed. These schemes will always exhibit a slight degree of stability for $\omega_1 = 0$, as in this case, the branch responsible for magnetization causes a short circuit in the rotor branch, as depicted in Figure 1. Consequently, the availability of speed information at the stator terminals is compromised. However, this predicament can be resolved when parasitic effects, such as rotor slot harmonics (this problem is resolved [12],[13],[14],[15]) or rotor saliencies [14],[16][17] are used to estimate speed. It is worth noting that the former tends to diminish with the implementation of skewed rotors, whereas extracting information from the latter becomes challenging unless deliberate measures are taken to enhance rotor saliency [18],[19], which is typically not feasible. Thus, further examination of parasitic effects will be abstained from in this paper.

D. DFO (Direct Field Orientation)

In a direct field orientation (DFO), a flux estimate $\hat{\psi}_R^s$ is straight calculated using the dynamic models in stator coordinates (eq.1) and (eq.2). The factor for d-q transformation can be computed in the manner described below.:

$$e^{-j\theta} = \frac{(\hat{\psi}_R^s)^*}{|\hat{\psi}_R^s|} \tag{5}$$

Figure 2 illustrates the schematic of a DFO. A drawback of DFO is that the frequency of stator, $\omega_1 = d\hat{\theta}/dt$, is not a well-defined variable; the quantities oscillate continuously in the steady state.

1. **CM (Current Model):** Simulating eq. (2) is a precise method for estimating the flux. Therefore:

$$\frac{d\hat{\psi}_R^s}{dt} = \hat{R}_R i_s^s - (\hat{a} - j\omega_r)\hat{\psi}_R^s \quad (6)$$

Where $\hat{a} = \hat{R}_R/\hat{L}_M$ and in cases where using model motor parameters—approximations that may not match their valid values—has been made clear (by hats). For all operating conditions, the (CM) can generate an asymptotically stable system, even when the parameters vary considerably[20],[21]. One drawback of this system is its sensitivity to parameters, particularly rotor resistance. This sensitivity results in a slower torque response when there are significant changes in the rotor resistance, denoted as $R_R - \tilde{R}_R$. The speed enters eq. (6) for a sensorless drive, and must be replaced by its estimated $\hat{\omega}_r$ in eq. (6), nonlinearity is introduced as

$$\hat{E}_s = \hat{R}_R i_s^s - [(\hat{a} - j\hat{\omega}_r)(\psi_R^s)]\hat{\psi}_R^s \quad (7)$$

One benefit of this is that the previously mentioned sensitivity to changes in the rotor resistance becomes negligible. The reasoning is that the stator terminals do not allow for the unique identification of the rotor speed and resistance (barring the injection of test signals or the application of parasitic effects). This can be inferred from the steady-state equivalent circuit [20],[22] where the equivalent resistance R_R/s , where $s = ((\omega_1 - \omega_r) / \omega_1)$ is the slip, replacing the series connection of R_R and the rotor EMF. in the rotor branch in Figure 1. Regrettably, the CM's desired stability characteristics are lost. If the CM is to be used in a sensorless drive, more investigation is required. In this regard, some findings are elaborated in the subsequent

2. **VM (Voltage Model) With Modifications:** A flux EMF is solvable through eq. (1) as

$$E^s = v_s^s - R_s i_s^s - L_\sigma \frac{di_s^s}{dt} \quad (8)$$

Thus, based on eq.(2), the flux can be calculated by integrating eq. (8) as

$$\frac{d\hat{\psi}_R^s}{dt} = v_s^s - \hat{R}_s i_s^s - \hat{L}_\sigma \frac{di_s^s}{dt} \quad (9)$$

where, $E_v^s = v_s^s - \hat{R}_s i_s^s - \hat{L}_\sigma \frac{di_s^s}{dt}$

Model parameters have replaced valid parameters once more. Because speed is missing in eq.(9) [14], the voltage model (VM) is, by definition, a sensorless flux estimator [23][24]. In the middle and high-speed ranges, the parameters sensitivity of the VM is modest. The only essential parameter is a resistance of a stator, that has an influence only at low speeds [11]. The leakage inductance is insignificant because an incorrect value does not affect torque. Because of the open-loop integration, the VM is only marginally stable [25]: $\hat{\psi}_R^s$ is not

present on the right side of the equation (9). As a result, the VM in its current condition cannot be used. In the usual change, a low-pass filter substitutes the open-loop integration.

$$\frac{d\hat{\psi}_R^s}{dt} = v_s^s - \hat{R}_s i_s^s - \hat{L}_\sigma \frac{di_s^s}{dt} - \alpha_v \hat{\psi}_R^s \quad (10)$$

where Preferred, the bandwidth changes in step with the stator frequency in a linear manner as $\alpha_v = \lambda|\omega_1|$, referred to as a programmable low-pass filter [11],[26],[27][28]); this causes flux estimation error to occur; this can be remedied by scaling the estimator output with the complex gain during steady state operation

$$\frac{j\omega_1 + \alpha_v}{j\omega_1} = 1 - j\lambda \text{sgn}(\omega_1) \quad (11)$$

In the context where the signum function is denoted by $\text{sgn}(\cdot)$, the flux estimator obtained is referred to as the "statically compensated VM" (SCVM). The SCVM's utility for sensorless operation at all speeds has been demonstrated [29],[30].

3. **Reduced-Order State Observers:** The feedback of flux-EMF difference can enhance the CM.

$$\begin{aligned} \tilde{E}^s &= E_v^s - E_c^s \\ &= v_s^s - (\hat{R}_s - \hat{R}_R) i_s^s + (\hat{a} - j\hat{\omega}_r) \hat{\psi}_R^s - \hat{L}_\sigma \frac{di_s^s}{dt} \end{aligned} \quad (12)$$

the variance of the two flux-EMF computations provided in eq. (7) and eq. (9) as

$$\frac{d\hat{\psi}_R^s}{dt} = E_c^s + \tilde{E}^s \quad (13)$$

This is called a reduced-order state observer[9],[31] because the stator equation (1) is only impliedly included. The observer design has two degrees of freedom because gain k is complex. One effective gain selection for censored drives is $k = 0$ in the low-speed region, increasing toward 1(as the speed increases), which successfully transitions the motor state from the CM to a location close to the VM. In [32], a flux estimator that resembles a reduced-order state observer is suggested. In this estimator, the CM to the VM is transitioned using an observer controller as a speed increased.

4. **Full-Order State Observers:** Simulating both eq.(1) and eq.(2) will estimate the stator current. The resulting "full-order state observer" [9],[33] uses both equations to use feedback on the current estimation error $\tilde{i}_s^s = i_s^s - \hat{i}_s^s$.

$$\frac{d\hat{i}_s^s}{dt} = \frac{1}{\hat{L}_\sigma} (v_s^s - \hat{R}_s \hat{i}_s^s - E_c^s) + K_1 \tilde{i}_s^s \quad (14)$$

$$\frac{d\hat{\psi}_R^s}{dt} = E_c^s + K_1 \tilde{i}_s^s \quad (15)$$

E_c^s is (in this case) reformulated as a function of \hat{i}_s^s rather than i_s^s . The choice of the two complex gains now has four degrees of freedom, which makes the design process more challenging. Regarding stability, the full-order state observer has no advantage over the reduced-order state observer [34],[35]; however, it generally rejects measurement disturbance more efficiently [36],[37].

5. **Speed Estimation:** A flux estimator in a sensorless drive must be supplemented with a speed estimator. Due to the consideration of ω_r , flux estimation relates to the estimation of states, whereas speed estimation is concerned with estimating parameters or adaptation[38]. The flux-EMF difference \tilde{E}^s can be incorporated into an integral adaptation law for the reduced-order observer[34], [39].

$$\frac{d\hat{\omega}_r}{dt} = I_m \{ K_\omega (\hat{\psi}_R^s) * \tilde{E}^s \} \quad (16)$$

Where, $K_\omega = K_\omega e^{-j\Omega}$, $K_\omega > 0$ is the complex adaptation gain. For the full-order state observer, a proportional-plus-integral adaptation law is frequently applied.

$$\hat{\omega}_r = K_p \varepsilon + K_i \int \varepsilon dt, \varepsilon = -I_m \{ e^{-j\phi} (\hat{\psi}_R^s) * \tilde{i}_s^s \}. \quad (17)$$

the nonnegative gains k_p and k_i chosed from a range of options deemed appropriate for achieving the desired dynamics properties; this will not affect the system's stability [35],[40],[41]. However, the rotation angle, where $\phi = 0$ leads to the conventional adaptation law [42],[43], significantly affects the stability characteristics.

6. **MRASs (Model-Reference Adaptive Systems):** However, a different strategy is to run a CM simultaneously and a modified version of a VM, yielding two kinds of flux estimates that can be denoted as $\hat{\psi}_R^{sc}$ and $\hat{\psi}_R^{sv}$, respectively [44],[45]. For field orientation, one of the two flux estimates is utilized. According to eq.(17), the speed estimate can be obtained, but with

$$\varepsilon = I_m \{ \hat{\psi}_R^{sc} (\hat{\psi}_R^{sv}) * \}. \quad (18)$$

The speed adaptation law effectively minimizes the angle difference between two flux estimates to zero. In the 1990s, it was discovered through thorough investigation that model-reference adaptive systems (MRASs) exhibited vulnerability to model parameter mistakes. Oscillations may become unstable or inadequately damped [45],[46],[47],[48].

7. **Relations Between the Schemes:** A flux estimator should be constructed in accordance with the model equation (1) and must adhere to the fundamental principles of the IM, regardless of the specific selection process as indicated by equation (2). Hence, it is unsurprising that the schemes as mentioned above exhibit interconnections. In [49],[50], It is demonstrated that the fundamental MRAS estimator can be obtained as a special case when the stator flux is selected as the first state variable in a full-order state observer, as opposed to the stator current . [51] make a comparison of two MRAS variants and a full-order observer while [52] and [53] contrast full-order state observers and naturally sensorless estimators. In [54],[55], present an analysis of the relationships between MRASs, reduced-order state observers, and full-order state observers. In [34], it is demonstrated how to convert a full-order state observer into an equivalent reduced-order state observer.

8. **Damping Estimator:** In order to mitigate the occurrence of parasitic oscillations, the estimator must possess a robust damping characteristic. These oscillations may arise due to inaccuracies in the model's parameters or discrete-time effects, particularly in a digital implementation. Due to the utilisation of open-loop integration in the unmodified virtual machine (VM), damping is absent. The estimator has inadequate damping characteristics at

higher velocities, despite the fact that the center of mass for filtered operation yields favorable stability qualities for the resultant closed-loop system. Despite the commendable stability attributes of the closed-loop system resulting from the use of the control module in filtered operation, it is seen that the estimator lacks sufficient damping characteristics at higher speeds. Equation (6) illustrates that, with the exception of the low-speed region, where the pole is located at $-a+j\omega_r$, the imaginary part is substantially more significant than the real part. In order to get satisfactory damping in full-order state observers, it is necessary to choose observer gains with sufficiently large real parts. As a result, the observer poles' actual components are significantly shifted towards the left half-plane. The process of amplifying signals with little noise is another design goal proposed in [56],[57].

E. IFO (Indirect Field Orientation)

Indirect field orientation (IFO) uses polar coordinates to calculate the flux estimate instead of direct field orientation (DFO), which uses Cartesian coordinates.

1) Standard IFO Using the CM

Converting the CM to polar coordinates led to the creation of the original IFO scheme, giving:

$$\begin{aligned}\frac{d\hat{\psi}_R e^{j\hat{\theta}}}{dt} &= \hat{R}_R i_s^s - (\hat{a} - j\hat{\omega}) \hat{\psi}_R e^{j\hat{\theta}} \\ \frac{d\hat{\psi}_R}{dt} + j \frac{d\hat{\theta}}{dt} \hat{\psi}_R &= \hat{R}_R i_s^s - (\hat{a} - j\hat{\omega}) \hat{\psi}_R\end{aligned}\quad (19)$$

The term $\frac{d\hat{\theta}}{dt}$ refers to stator frequency. The following relations (eq.20 & eq.21) result from breaking down equation (19) into its real and imaginary components:

$$\frac{d\hat{\psi}_R}{dt} = \hat{R}_R i_d - \hat{a} \hat{\psi}_R \quad (20)$$

$$\frac{d\hat{\theta}}{dt} = \omega_1 = \hat{\omega}_R + \frac{\hat{R}_R i_d}{\hat{\psi}_R} \quad (21)$$

Equation (20) indicates the ψ_R converges to $\hat{L}_M i_d$ with the time constant $1/\hat{a}$. It follows that the stator current needs to be regulated in a way that

$$i_d = \frac{\psi_{ref}}{\hat{L}_M} \quad (22)$$

The slip relation, or equation (21), shows the electrical rotor speed and the slip frequency. $\hat{R}_R i_d / \hat{\psi}_R$ equals the stator frequency. The estimation of IFO flux is conducted in the d-q frame, in contrast to DFO, where all variables remain constant during the steady state. This confers a number of benefits. The control algorithm incorporates the stator frequency as an explicit variable, which provides an additional advantage. Another advantage lies in the fact that the issue of poor damping in the estimator is mitigated to a lesser extent. Although the estimator proposed in [42],[58] provides an estimate of the α - β frame flux, the integrated Clarke's transformation is employed in the dq frame to address the insufficient damping observed at higher velocities, as discussed before. One potential limitation of IFO is the necessity to compute sine and cosine during the dq transformation process. However, it is worth noting that contemporary state-of-the-art digital implementation methods can efficiently and cost-effectively fulfill this computational requirement.

2) Generalized IFO

In previous times, the concept of the CM was widely regarded as the sole flux estimator possessing an IFO implementation of a comparable nature. Conversely, a corresponding application of the IFO may be found for every DFO flux estimator [59]. As an illustration, the VM in eq. (9) is changed to

$$\frac{d\hat{\psi}_R}{dt} + j \frac{d\hat{\theta}}{dt} \hat{\psi}_R = v_s - \hat{R}_s i_s - j\omega_1 \hat{L}_\sigma i_s - \hat{L}_\sigma \frac{di_s}{dt} \quad (23)$$

The solution for the real and imaginary components (for eq.23) can be derived from this equation.

$$\frac{d\hat{\psi}_R}{dt} = v_d - \hat{R}_s i_d + \omega_1 \hat{L}_\sigma i_q - \hat{L}_\sigma \frac{di_d}{dt} \quad (24)$$

$$\frac{d\hat{\theta}}{dt} = \omega_1 = v_q - \hat{R}_s i_q - \omega_1 \hat{L}_\sigma i_d - \hat{L}_\sigma \frac{di_q}{dt} \quad (25)$$

The stator current exhibits a higher variation rate than the rotor flux, thereby rendering the stator-current derivatives on the right-hand sides of equations (24) and (25) frequently negligible. There is the option to either solve for ω_1 or integrate the right side into a low-pass filter [60],[61] can be applied to break the algebraic loop that is produced when 1 appears on both sides of the equation (25). It should be noted that although the CM's equations (20) and (21) have the same purposes, equations (24) and (25) differ significantly. Equation (25) is introduced as a replacement for the slip relation in the context of the CM.

3) Non-DFO-Corresponding Modifications

The conversion of all DFO Flux estimators to their corresponding IFO estimators is possible. However, it should be noted that certain IFO Flux estimators do not have matching DFO counterparts. Performance can be improved by making adjustments to an IFO that is equivalent to a DFO flux estimator. A low-pass filter can effectively address the open-loop integration described in equation (24). However, unlike equation (10), which does not consider the Flux reference in the extra term, incorporating it as indicated in references [62],[63], it is reasonably simple to prevent an estimation error

$$\frac{d\hat{\psi}_R}{dt} = v_d - \hat{R}_s i_d + \omega_1 \hat{L}_\sigma i_q + \alpha_v (\psi_{ref} - \hat{\psi}_R) \quad (26)$$

A further illustration can be observed in modifying SCVM proposed in [60].

4) Transitioning to an Essentially Sensorless System

The process outlined in this study can be employed to construct an IFO flux estimator, which inherently lacks sensorless capabilities [64]. It is recommended to utilize the IFO version of the speed adaption law, as depicted by equation 16.

$$\frac{d\hat{\omega}_r}{dt} = I_m \{K_\omega \hat{\psi}_R \tilde{E}\} \quad (27)$$

where \tilde{E} is acquired through the d-q transformation of eq.(12)

$$\tilde{E} = v_s - (\hat{R}_s + \hat{R}_R + j\omega_1 \hat{L}_\sigma) i_s + (\hat{a} - j\hat{\omega}) \hat{\psi}_R \quad (28)$$

By neglecting di_s/dt . Assume, for instance, that k_ω is chosen real value,

$k\omega = k_\omega$, such is the yield.

$$\frac{d\hat{\omega}_r}{dt} = K_\omega \hat{\psi}_R [v_q - (\hat{R}_s + \hat{R}_R) i_q + \omega_1 \hat{L}_\sigma i_d - \hat{\omega}_r \hat{\psi}_R] \quad (29)$$

The negative value of the coefficient for ω_r on the right side of equation (29) signifies that the speed estimator is approximately stable. As the value of k_ω increases, $\hat{\omega}_r$ will converge considerably faster than the flux, resulting in the flux estimator noting that $d\hat{\omega}_r/dt = 0$. This enables the solution of $\hat{\omega}_r$ via the right side of (29), which yields

$$\hat{\omega}_r = \frac{v_q - (\hat{R}_s + \hat{R}_R) i_q + \omega_1 \hat{L}_\sigma i_d}{\hat{\psi}_R} \quad (30)$$

By substituting in eq. (21), This term can now be employed to make the IFO-CM fundamentally sensorless

$$\begin{aligned} \omega_1 &= \frac{v_q - (\hat{R}_s + \hat{R}_R) i_q + \omega_1 \hat{L}_\sigma i_d}{\hat{\psi}_R} + \frac{\hat{R}_R i_q}{\hat{\psi}_R} \\ &= \frac{v_q - \hat{R}_s i_q + \omega_1 \hat{L}_\sigma i_d}{\hat{\psi}_R} \end{aligned} \quad (31)$$

Significantly, the CM undergoes a partial transformation into the VM, simplifying equation (25) when the rate of change of di_q/dt is disregarded. This partial transformation occurs due to the discrepancy between equation (20) and equation (24). This analysis illustrates the distinct dynamic characteristics and parameter sensitivity exhibited by the sensorless condition monitoring (CM) compared to the censored CM. In [35], a similar estimator is taken into account. For a complex $k\omega$, a different result is obtained, but the result is still an intrinsically sensorless flux estimator.

5) Estimation of Speed via an Inherently Sensorless System

One of the benefits of utilizing a sensorless Indirect Field-Oriented (IFO) system is the simplification of speed estimate to the use of a backward-applied slip relation. The speed estimate can be calculated via equation (21), provided that the generalized slip relation yields a value of ω_1 .

$$\hat{\omega}_R = \omega_1 - \frac{\hat{R}_R i_q}{\hat{\psi}_R} \quad (32)$$

6) Rotor-Resistance Estimation

Recall that in a sensorless drive, the flux estimate is unaffected by the rotor resistance. The \hat{R}_R terms cancel in eq. (31) where this is explicitly observed. However, it is noted in eq. (32), even in the steady state, that \hat{R}_R not equal R_R causes an erroneous estimate of the slip frequency and, as a result, an error in the speed estimation. Rotor resistance estimation in a sensorless drive is therefore desirable but difficult. In the analogous steady-state circuit [23], an equivalent resistance R_R/S , where $S = (\omega_1 - \omega_r) / \omega_1$ is the slip, is used in place of the series connection

of R_R and the rotor EMF $j\omega_r\psi_R^S$ in the rotor branch in Figure 1. As a result, it can be inferred that it is impossible to estimate speed and rotor resistance simultaneously in the steady state. This deduction is supported by observability analysis[65],[66]. It is necessary to resort to transients, harmonics, or injected signals[67],[47].

6. Discussion

In this section, some techniques used for stabilizing sensorless induction motor drives discussed. In [61], Extended Kalman Filter (EKF) presents a solid foundation for sensorless control, though computational efficiency is a concern for real-time applications. The technique in [68] is Sliding Mode Observer showed effectiveness in enhancing system stability. In [69], MRAS with genetic Algorithm (GA) Optimization are used, which showed effectiveness in dynamically tuning the PI controller for optimal performance. And for [70], the technique is High-Frequency Signal Injection (HF), which showed effectiveness in detecting rotor position with minimal estimation error, emphasizing its superiority in sensorless control. Table 1. summarizes these techniques used for stabilizing sensorless induction motor drives, aided by the weaknesses, main contributions, and strengths.

Table 1. Summary of the properties for some techniques used for stabilizing sensorless induction motor drives.

Reference	techniques	main contributions	strengths	weaknesses
[61]	Extended Kalman Filter (EKF)	1. Robust estimation of states and parameters under model uncertainties 2. Widely applied in sensorless control	1. Good performance in nonlinear systems 2. Can handle noisy measurements	1. High computational complexity 2. Sensitivity to model parameters
[68]	Sliding Mode Observer	Robust estimation under parameter uncertainties	High accuracy and robustness against disturbances	Potential for chattering
[69]	MRAS with GA Optimization	Enhanced adaptation mechanism with optimized PI controller parameters	Robust performance in dynamic system variations	Computational complexity
[70]	High-Frequency Signal Injection (HF)	1. Effective in both synchronous and asynchronous machines 2. Utilizes rotor slotting and magnetic core saturation asymmetries for rotor position detection	1. High accuracy in rotor position estimation 2. Applicable across a range of speed	1. Complexity in implementation 2. Potential interference with signal processing

7. Conclusion

In this article, the sensorless methodologies and principles utilized in the stabilization control of induction motor (IM) drives are exhaustively examined. In order to successfully develop a sensorless control system, it is essential to have a comprehensive understanding of electrical motor and drives, in addition to systems and control theories. Flux estimation is an indispensable component of these control systems. Despite the strong preference for minimal complexity estimators, the selection of an estimator does not serve as the principal determinant. Nevertheless, the central emphasis is on the analytical ascertainment of the estimator gains in order to effectively mitigate and prevent the occurrence of instability. Significant progress has been achieved in the area of sensorless operation stability at moderate speeds since the turn of the millennium. To enhance the stabilization and control of sensorless induction motor (IM) drives, several features can be recommended based on the techniques discussed and the specifics of their application environments. These features aim to address common challenges such as parameter variations, low-speed operation, and computational efficiency by using Adaptive Parameter Estimation, Advanced Filtering and Noise Reduction, and Hybrid Estimation Strategies which offers a versatile and robust solution that can adapt to various scenarios, ensuring optimal performance across the entire speed range.

References

- [1] M. Popescu, *Induction motor modelling for vector control purposes*. 2000.
- [2] M. Ranta and M. Hinkkanen, "Online identification of parameters defining the saturation characteristics of induction machines," *IEEE Trans. Ind. Appl.*, vol. 49, no. 5, pp. 2136–2145, 2013, doi: 10.1109/TIA.2013.2261793.
- [3] Z. Q. Zhu, D. Liang, and K. Liu, "Online Parameter Estimation for Permanent Magnet Synchronous Machines: An Overview," *IEEE Access*, vol. 9, pp. 59059–59084, 2021, doi: 10.1109/ACCESS.2021.3072959.
- [4] L. Harnefors and M. Hinkkanen, "Stabilization of sensorless induction motor drives: A survey," *Proc. - 2013 IEEE Work. Electr. Mach. Des. Control Diagnosis, WEMDCD 2013*, pp. 183–192, 2013, doi: 10.1109/WEMDCD.2013.6525178.
- [5] L. Harnefors and H. P. Nee, "Model-based current control of ac machines using the internal model control method," *IEEE Trans. Ind. Appl.*, vol. 34, no. 1, pp. 133–141, 1998, doi: 10.1109/28.658735.
- [6] F. Jiang *et al.*, "Robustness Improvement of Model-Based Sensorless SPMSM Drivers Based on an Adaptive Extended State Observer and an Enhanced Quadrature PLL," *IEEE Trans. Power Electron.*, vol. 36, no. 4, pp. 4802–4814, 2021, doi: 10.1109/TPEL.2020.3019533.
- [7] Z. M. A. and A. A. Z. D. Ahmed G. Mahmoud A. Aziz , Almoataz Y. Abdelaziz, "A Comprehensive Examination of Vector-Controlled Induction Motor Drive Techniques," 2023, doi: 10.3390/en16062854.
- [8] "The Field Orientation Principle in Control of Induction Motors THE KLUWER INTERNATIONAL SERIES."
- [9] G. C. Verghese and S. R. Sanders, "Observers For Flux Estimation In Induction Machines," *IEEE Trans. Ind. Electron.*, vol. 35, no. 1, pp. 85–94, 1988, doi: 10.1109/41.3067.
- [10] C. J. V. Filho, D. Xiao, R. P. Vieira, and A. Emadi, "Observers for High-Speed Sensorless PMSM Drives: Design Methods, Tuning Challenges and Future Trends," *IEEE Access*, vol. 9, pp. 56397–

56415, 2021, doi: 10.1109/ACCESS.2021.3072360.

- [11] L. Harnefors, "Design and analysis of general rotor-flux-oriented vector control systems," *IEEE Trans. Ind. Electron.*, vol. 48, no. 2, pp. 383–390, 2001, doi: 10.1109/41.915417.
- [12] R. Biasco-Gimenez, G. M. Asher, M. Summer, and K. J. Bradley, "Performance of FFT-rotor slot harmonic speed detector for sensorless induction motor drives," *IEE Proc. Electr. Power Appl.*, vol. 143, no. 3, pp. 258–267, 1996, doi: 10.1049/ip-epa:19960241.
- [13] W. L. Silva, A. M. N. Lima, and A. Oliveira, "Speed Estimation of an Induction Motor Operating in the Nonstationary Mode by Using Rotor Slot Harmonics," *IEEE Trans. Instrum. Meas.*, vol. 64, no. 4, pp. 984–994, 2015, doi: 10.1109/TIM.2014.2361554.
- [14] M. Hilairet and F. Auger, "Sensorless speed measurement using current harmonic spectral estimation in a DC-motor," *Int. Symp. Power Electron. Electr. Drives, Autom. Motion, 2006. SPEEDAM 2006*, vol. 2006, no. 1, pp. 740–745, 2006, doi: 10.1109/SPEEDAM.2006.1649867.
- [15] J. Bonet-Jara and J. Pons-Llinares, "A Precise, General, Non-Invasive and Automatic Speed Estimation Method for MCSA Diagnosis and Efficiency Estimation of Induction Motors," *IEEE Trans. Energy Convers.*, vol. 38, no. 2, pp. 1257–1267, 2023, doi: 10.1109/TEC.2022.3220853.
- [16] Y. gu Kang, D. Fernandez, and D. D. Reigosa, "Saliency-Based Rotor Spatial Position Displacement Self-Sensing for Self-Bearing Machines," *Sensors*, vol. 22, no. 24, pp. 1–18, 2022, doi: 10.3390/s22249663.
- [17] Y. Li, H. Wu, X. Xu, X. Sun, and J. Zhao, "Rotor position estimation approaches for sensorless control of permanent magnet traction motor in electric vehicles: A review," *World Electr. Veh. J.*, vol. 12, no. 1, pp. 1–26, 2021, doi: 10.3390/WEVJ12010009.
- [18] P. L. Jansen and R. D. Lorenz, "Transducerless Position and Velocity Estimation in Induction and Salient AC Machines," *IEEE Trans. Ind. Appl.*, vol. 31, no. 2, pp. 240–247, 1995, doi: 10.1109/28.370269.
- [19] J. Y. Chen and S. C. Yang, "Saliency-Based Permanent Magnet Machine Position Sensorless Drive Using Proposed PWM Injection and Shunt-Based Current Sensing for Position Estimation," *IEEE Trans. Ind. Electron.*, vol. 68, no. 7, pp. 5693–5703, 2021, doi: 10.1109/TIE.2020.3000088.
- [20] P. A. S. De Wit, R. Ortega, and I. Mareels, "Indirect field-oriented control of induction motors is robustly globally stable," *Automatica*, vol. 32, no. 10, pp. 1393–1402, 1996, doi: 10.1016/0005-1098(96)00070-2.
- [21] R. J. Wai and K. M. Lin, "Robust decoupled control of direct field-oriented induction motor drive," *IEEE Trans. Ind. Electron.*, vol. 52, no. 3, pp. 837–854, 2005, doi: 10.1109/TIE.2005.847585.
- [22] R. Ortega, B. Yi, and J. G. Romero, "Robustification of nonlinear control systems vis-à-vis actuator dynamics: An immersion and invariance approach," *Syst. Control Lett.*, vol. 146, p. 104811, 2020, doi: 10.1016/j.sysconle.2020.104811.
- [23] B. Bose, "Power Electronics and Motor Drives," *Power Electron. Mot. Drives*, vol. 56, no. 2, pp. 581–588, 2006, doi: 10.1016/B978-0-12-088405-6.X5000-6.
- [24] I. N. Jiya and R. Gouws, "Overview of power electronic switches: A summary of the past, state-of-the-art and illumination of the future," *Micromachines*, vol. 11, no. 12, pp. 1–29, 2020, doi: 10.3390/mi11121116.
- [25] P. Shrawane, "Indirect field - Oriented Control of Induction motor," *Int. Power Electron. Congr. - CIEP*, pp. 102–105, 2010, doi: 10.1109/CIEP.2010.5598838.
- [26] A. Boudallaa, M. Chennani, D. Belkhat, and K. Rhofir, "Vector Control of Asynchronous Motor of Drive Train Using Speed Controller H_∞ ," *Emerg. Sci. J.*, vol. 6, no. 4, pp. 834–850, 2022, doi: 10.28991/ESJ-2022-06-04-012.

- [27] I. Takahashi and T. Noguchi, "A New Quick-Response and High-Efficiency Control Strategy of an Induction Motor," *IEEE Trans. Ind. Appl.*, vol. IA-22, no. 5, pp. 820–827, 1986, doi: 10.1109/TIA.1986.4504799.
- [28] F. Farhani, A. Zaafour, and A. Chaari, "Real time induction motor efficiency optimization," *J. Franklin Inst.*, vol. 354, no. 8, pp. 3289–3304, 2017, doi: 10.1016/j.jfranklin.2017.02.012.
- [29] U. Baader, M. Depenbrock, and G. Gierse, "Direct self control of inverter-fed induction machine, a basis for speed control without speed-measurement," *Conf. Rec. - IAS Annu. Meet. (IEEE Ind. Appl. Soc.)*, vol. 28, no. pt 1, pp. 486–492, 1989, doi: 10.1109/ias.1989.96695.
- [30] B. R. Vinod and G. Shiny, "Direct Torque Control Scheme for a Four-Level-Inverter Fed Open-End-Winding Induction Motor," *IEEE Trans. Energy Convers.*, vol. 34, no. 4, pp. 2209–2217, 2019, doi: 10.1109/TEC.2019.2941890.
- [31] M. Morawiec, P. Kroplewski, and C. Odeh, "Nonadaptive Rotor Speed Estimation of Induction Machine in an Adaptive Full-Order Observer," *IEEE Trans. Ind. Electron.*, vol. 69, no. 3, pp. 2333–2344, 2022, doi: 10.1109/TIE.2021.3066919.
- [32] B. K. Bose and N. R. Patel, "A programmable cascaded low-pass filter-based flux synthesis for a stator flux-oriented vector-controlled induction motor drive," *IEEE Trans. Ind. Electron.*, vol. 44, no. 1, pp. 140–143, 1997, doi: 10.1109/41.557511.
- [33] Y. Wang, S. Tobayashi, and R. D. Lorenz, "A Low-Switching-Frequency Flux Observer and Torque Model of Deadbeat-Direct Torque and Flux Control on Induction Machine Drives," *IEEE Trans. Ind. Appl.*, vol. 51, no. 3, pp. 2255–2267, 2015, doi: 10.1109/TIA.2014.2365628.
- [34] M. H. Shin, D. S. Hyun, S. B. Cho, and S. Y. Choe, "An improved stator flux estimation for speed sensorless stator flux orientation control of induction motors," *IEEE Trans. Power Electron.*, vol. 15, no. 2, pp. 312–318, 2000, doi: 10.1109/63.838104.
- [35] A. Venkatesh, "An Improved Adaptive Smo for Speed Estimation of Sensorless Dsfoe Induction Motor Drives and Stability Analysis using Lyapunov Theorem at Low Frequencies," *Int. J. Eng. Res.*, vol. V8, no. 09, pp. 246–253, 2019, doi: 10.17577/ijertv8is090020.
- [36] L. Harnefors, M. Jansson, R. Ottersten, and K. Pietiläinen, "Unified sensorless vector control of synchronous and induction motors," *IEEE Trans. Ind. Electron.*, vol. 50, no. 1, pp. 153–160, 2003, doi: 10.1109/TIE.2002.807653.
- [37] B. Wang, J. Zhang, Y. Yu, X. Zhang, and D. Xu, "Unified Complex Vector Field-Weakening Control for Induction Motor High-Speed Drives," *IEEE Trans. Power Electron.*, vol. 36, no. 6, pp. 7000–7011, 2021, doi: 10.1109/TPEL.2020.3034246.
- [38] V. Tiwari, S. Das, and A. Pal, "Sensorless speed control of induction motor drive using extended Kalman filter observer," *Asia-Pacific Power Energy Eng. Conf. APPEEC*, vol. 2017-Novem, pp. 1–6, 2017, doi: 10.1109/APPEEC.2017.8308989.
- [39] O. E. M. Youssef, M. G. Hussien, and A. E. W. Hassan, "A new simplified sensorless direct stator field-oriented control of induction motor drives," *Front. Energy Res.*, vol. 10, no. September, pp. 1–8, 2022, doi: 10.3389/fenrg.2022.961529.
- [40] L. Harnefors and M. Hinkkanen, "Complete stability of reduced-order and full-order observers for sensorless IM drives," *IEEE Trans. Ind. Electron.*, vol. 55, no. 3, pp. 1319–1329, 2008, doi: 10.1109/TIE.2007.909077.
- [41] J. Ji, Y. Jiang, W. Zhao, Q. Chen, and A. Yang, "Sensorless Control of Linear Vernier Permanent-Magnet Motor Based on Improved Mover Flux Observer," *IEEE Trans. Power Electron.*, vol. 35, no. 4, pp. 3869–3877, 2020, doi: 10.1109/TPEL.2019.2934984.
- [42] P. L. Jansen and R. D. Lorenz, "A Physically Insightful Approach to the Design and Accuracy Assessment of Flux Observers for Field Oriented Induction Machine Drives," *IEEE Trans. Ind.*

- Appl.*, vol. 30, no. 1, pp. 101–110, 1993, doi: 10.1109/28.273627.
- [43] S. M. Peresada, S. M. Kovbasa, O. V Statsenko, and O. V Serhiienko, “controller design and experimental robustness evaluation,” vol. 5, no. 3, pp. 217–227, 2022.
- [44] T. Tuovinen, M. Hinkkanen, L. Harnefors, and S. Member, “Comparison of a Reduced-Order Observer and a Full-Order Observer for Sensorless Synchronous Motor Drives,” 2012, doi: 10.1109/tia.2012.2226200.Title.
- [45] T. Orłowska-Kowalska, M. Korzonek, and G. Tarchala, “Stability Improvement Methods of the Adaptive Full-Order Observer for Sensorless Induction Motor Drive-Comparative Study,” *IEEE Trans. Ind. Informatics*, vol. 15, no. 11, pp. 6114–6126, 2019, doi: 10.1109/TII.2019.2930465.
- [46] R. S. McNair, “Triage,” *Rapid Access Guid. Triage Emerg. Nurses Chief Complain. with High-Risk Present. Second Ed.*, vol. 1, no. 4, pp. 8–19, 2023, doi: 10.1891/9780826169761.0002.
- [47] H. Kubota, K. Matsuse, and T. Nakano, “DSP-Based Speed Adaptive Flux Observer of Induction Motor,” *IEEE Trans. Ind. Appl.*, vol. 29, no. 2, pp. 344–348, 1993, doi: 10.1109/28.216542.
- [48] Z. Tir, T. Orłowska-Kowalska, H. Ahmed, and A. Houari, “Adaptive High Gain Observer Based MRAS for Sensorless Induction Motor Drives,” *IEEE Trans. Ind. Electron.*, vol. 71, no. 1, pp. 271–281, 2024, doi: 10.1109/TIE.2023.3243271.
- [49] M. Hinkkanen and J. Luomi, “Stabilization of regenerating-mode operation in sensorless induction motor drives by full-order flux observer design,” *IEEE Trans. Ind. Electron.*, vol. 51, no. 6, pp. 1318–1328, 2004, doi: 10.1109/TIE.2004.837902.
- [50] M. S. Zaky, “Stability analysis of speed and stator resistance estimators for sensorless induction motor drives,” *IEEE Trans. Ind. Electron.*, vol. 59, no. 2, pp. 858–870, 2012, doi: 10.1109/TIE.2011.2161658.
- [51] C. Schauder, “Adaptive Speed Identification for Vector Control of Induction Motors Without Rotational Transducers,” *IEEE Trans. Ind. Appl.*, vol. 28, no. 5, pp. 1054–1061, 1992, doi: 10.1109/28.158829.
- [52] R. Biasco-Giménez, “Dynamic performance limitations for MRAS based sensorless induction motor drives. Part 1: Stability analysis for the closed loop drive,” *IEE Proc. Electr. Power Appl.*, vol. 143, no. 2, pp. 113–121, 1996, doi: 10.1049/ip-epa:19960104.
- [53] R. S. I. Drive, “Stator-Current-Based MRAS Estimator for a Wide,” *IEEE Trans. Ind. Electron.*, vol. 57, no. 4, pp. 1296–1308, 2010.
- [54] R. Biasco-Giménez, “Dynamic performance limitations for MRAS based sensorless induction motor drives. Part 2: Online parameter tuning and dynamic performance studies,” *IEE Proc. Electr. Power Appl.*, vol. 143, no. 2, pp. 123–134, 1996, doi: 10.1049/ip-epa:19960105.
- [55] S. M. Gadoue, D. Giaouris, and J. W. Finch, “Sensorless control of induction motor drives at very low and zero speeds using neural network flux observers,” *IEEE Trans. Ind. Electron.*, vol. 56, no. 8, pp. 3029–3039, 2009, doi: 10.1109/TIE.2009.2024665.
- [56] M. Hinkkanen, “Analysis and design of full-order flux observers for sensorless induction motors,” *IEEE Trans. Ind. Electron.*, vol. 51, no. 5, pp. 1033–1040, 2004, doi: 10.1109/TIE.2004.834964.
- [57] G. Brando, A. Dannier, and I. Spina, “Performance analysis of a full order sensorless control adaptive observer for doubly-fed induction generator in grid connected operation,” *Energies*, vol. 14, no. 5, 2021, doi: 10.3390/en14051254.
- [58] O. Wallscheid and E. F. B. Ngoumtsa, “Investigation of Disturbance Observers for Model Predictive Current Control in Electric Drives,” *IEEE Trans. Power Electron.*, vol. 35, no. 12, pp. 13563–13572, 2020, doi: 10.1109/TPEL.2020.2992784.
- [59] B. K. Rose, “Power Electronics, Smart Grid and Renewable Energy Systems,” *Proc. IEEE*, vol. 105, no. 11, pp. 2007–2010, 2017, [Online]. Available:

<http://ieeexplore.ieee.org/abstract/document/8038782/>.

- [60] K. Ohyama, G. M. Asher, and M. Sumner, "Comparative analysis of experimental performance and stability of sensorless induction motor drives," *IEEE Trans. Ind. Electron.*, vol. 53, no. 1, pp. 178–186, 2006, doi: 10.1109/TIE.2005.862298.
- [61] R. Yildiz, M. Barut, and E. Zerdali, "A Comprehensive Comparison of Extended and Unscented Kalman Filters for Speed-Sensorless Control Applications of Induction Motors," *IEEE Trans. Ind. Informatics*, vol. 16, no. 10, pp. 6423–6432, 2020, doi: 10.1109/TII.2020.2964876.
- [62] J. Holtz and J. Quan, "Sensorless vector control of induction motors at very low speed using a nonlinear inverter model and parameter identification," *IEEE Trans. Ind. Appl.*, vol. 38, no. 4, pp. 1087–1095, 2002, doi: 10.1109/TIA.2002.800779.
- [63] Y. Guo, H. Wang, and T. Su, "Extremely low speed performance research of the speed sensorless vector controlled induction motor drive system," *IET Power Electron.*, vol. 15, no. 13, pp. 1441–1449, 2022, doi: 10.1049/pel2.12306.
- [64] Y. Cui and K. Wang, "Speed sensorless adaptive rotor flux orientation control of induction motor drive," 2023.
- [65] M. Koteich, A. Maloum, G. Duc, and G. Sandou, "Discussion on 'AC Drive Observability Analysis,'" *IEEE Trans. Ind. Electron.*, vol. 62, no. 11, pp. 7224–7225, 2015, doi: 10.1109/TIE.2015.2438777.
- [66] F. Boussekra and A. Makouf, "Sensorless Speed Control of IPMSM Using Sliding Mode Observer Based on Active Flux Concept," *Model. Meas. Control A*, vol. 93, no. 1–4, pp. 1–9, 2020, doi: 10.18280/mmc_a.931-401.
- [67] B. Rached, M. Elharoussi, E. Abdelmounim, and M. Bensaid, "Design and DSP implementation in HIL of nonlinear observers for a doubly fed induction aero-generator," *Bull. Electr. Eng. Informatics*, vol. 12, no. 3, pp. 1340–1351, 2023, doi: 10.11591/eei.v12i3.4562.
- [68] H. Che, B. Wu, J. Yang, and Y. Tian, "Speed sensorless sliding mode control of induction motor based on genetic algorithm optimization," *Meas. Control (United Kingdom)*, vol. 53, no. 1–2, pp. 192–204, 2020, doi: 10.1177/0020294019881711.
- [69] N. El Ouanjli, S. Mahfoud, M. S. Bhaskar, S. El Daoudi, A. Derouich, and M. El Mahfoud, "A new intelligent adaptation mechanism of MRAS based on a genetic algorithm applied to speed sensorless direct torque control for induction motor," *Int. J. Dyn. Control*, vol. 10, no. 6, pp. 2095–2110, 2022, doi: 10.1007/s40435-022-00947-z.
- [70] M. Duhancik, T. Coranic, S. Gaspar, and V. Lipovsky, "Sensorless Control Analysis of Electric Motor Drives Based on High-Frequency Signal Injection and Its Simulation Verification," *Actuators*, vol. 11, no. 11, 2022, doi: 10.3390/act11110317.

مراجعة تقنيات الاستقرار لمسوحات المحرك الحثي بدون حساسات

الخلاصة: التحديات التي تكمن في تحقيق الاستقرار في المحركات الحثية (IM) التي لا تحتوي على أجهزة استشعار أكثر بكثير من تلك التي تواجهها المحركات التي تحتوي على أجهزة استشعار. تغطي هذه المقالة بشكل شامل مقدرات التدفق والسرعة الموصى بها بشكل متكرر، بما في ذلك أجهزة مراقبة الحالة منخفضة الرتبة وأجهزة مراقبة حالة النظام بالكامل. الحساسية لتغيرات المعلمات (او المعاملات) والخصائص الثابتة والديناميكية هي محور البحث. يكون عدم الاستقرار أكثر حدة عند السرعات القليلة، مما يجعل مقاومة الجزء الثابت أهم عامل في هذا الاستطلاع، سيتم فحص الأساليب المختلفة للتخفيف من تأثيرات هذا العامل بالذات.

الكلمات المفتاحية: تقدير، المحرك الحثي، المراقبين، بدون مستشعر، استقرار.